Seasonal Wave Forecasting for Hawaii

Ning Li[*1], Sen Zhao[2], Kwok Fai Cheung[1], Fei-Fei Jin[2], Zhaoqing Yang[3]

[1]Department of Ocean and Resources Engineering, University of Hawaii at Manoa, Honolulu, HI 96822, USA
[2]Department of Atmospheric Sciences, University of Hawaii at Manoa, Honolulu, HI 96822, USA
[3]Marine Sciences Laboratory, Pacific Northwest National Laboratory, Seattle, WA 98109, USA
[*] Email: ningli@hawaii.edu

1 Background

The complex wave climate in Hawaii includes the year-round trade wind seas from the east and swells generated by extratropical cyclones in the North and South Pacific, as well as waves of variable direction from subtropical and tropical systems passing nearby. To resolve the diverse wave conditions, we assembled a numerical wave model system with the third-generation spectral wave model WAVEWATCH III [1] and SWAN [2] on a telescopic nested grid system from the globe to Hawaii. The surface wind reanalysis from the Climate Forecast System[3] [4] for the entire globe and its downscaling by the Weather Research and Forecasting model (WRF) [5] for the Hawaii region [6] were utilized as input forcing to produce a wave hindcast from 1980 to 2020. The 42 years of hindcast, with grid resolution reaching 300 m in nearshore regions around Hawaii, was thoroughly validated by the buoy measurements and satellite altimetry [7]. The validated hindcast dataset has been widely used in energy resources assessments, and wave climate, shoreline change, and coral reef ecosystem studies. We also operate the model system with surface winds from Global Forecast System and its regional downscaling for Hawaii to provide daily wave predictions for up to 14 days. This short-term prediction provides vital information for at-sea operations and day-to-day coastal activities [https://www.pacioos.hawaii.edu/waves-category/model/]. Major operations and coastal management also need forecast information in an extended range, such as seasonal scales, for better planning and preparation.

The goal of the seasonal wave forecast is not to predict the timing of wave activities but rather to estimate the overall sea states that are likely to be most prevalent over the coming season. Over decades of research, El Niño-Southern Oscillation (ENSO) has emerged as the primary driver for global seasonal climate forecasts. Previous studies, based on a low-resolution global wave hindcast [8–10], have demonstrated significant impacts of El Niño on Hawaii's wave climate. But, the orographic effect of the airflow and island sheltering of the multi-modal seas can only be resolved with high-resolution wave data. In this study, we used the 42 years of high-resolution hindcast to explore ENSO's modulation on Hawaii's coastal wave activities and developed an ENSO-based wave model to provide seasonal forecasts.

2 ENSO's modulation on seasonal wave statistics

The 42-year high-resolution wave hindcast reveals pronounced seasonality and distinct spatial patterns of wave statistics around the Hawaiian Islands. As illustrated in Figure 1, the monthly mean significant wave height (H_s^m) ranges from 1.0 to 1.5 m for the extended summer months from May to September, demonstrating mild and steady seas. In contrast, waves are more energetic in winter, with the mean Hs from November to March exceeding 3 m to the north. This drastic increase in wave heights is associated with the transition of dominant wave components—from trade wind waves in summer to north swells in winter. Shadowing effects near the southeast and west shores occur due to the sheltering of north swells and, to a lesser extent, easterly wind waves.

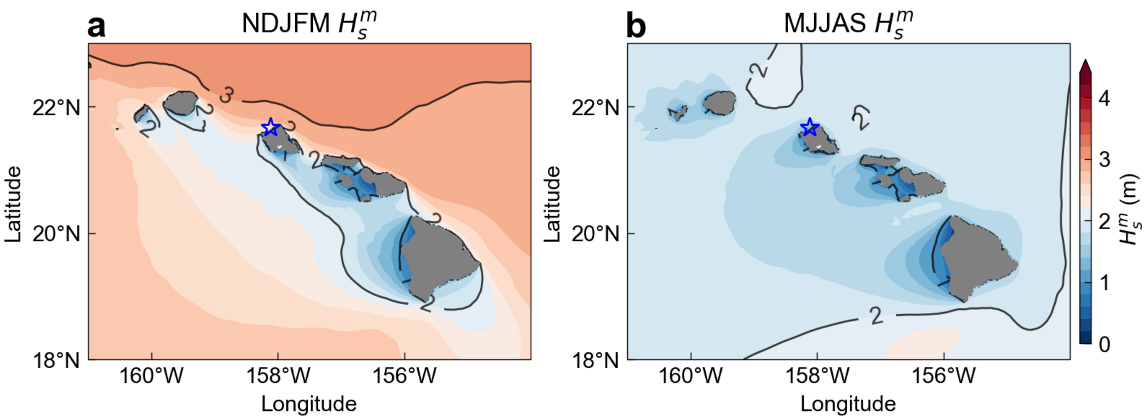

Figure 1. Seasonal climatological statistics of mean Hs around the Hawaiian Islands. (a) May to September; (b) November to March. The blue star marks buoy #106.

Despite significant seasonal variations in wave activities, the strong influence of ENSO on Hawaiian waves is evident in the correlation between the Niño3.4 index and H_s^m (Figure 2). During the winter months, the correlation coefficient exceeds 0.8 at the north and west shores, which are exposed to north swells, indicating the strong modulation of ENSO on swell amplitudes. In the summer months, the ENSO-wave correlation is relatively small, indicating that the east trade wind waves are less responsive to ENSO than the north swells. The dramatic transition of ENSO impacts on local wave activities from winter to summer highlights the crucial role of the seasonal cycle in modulating the inter-annual relationship between ENSO and ocean waves or vice versa.

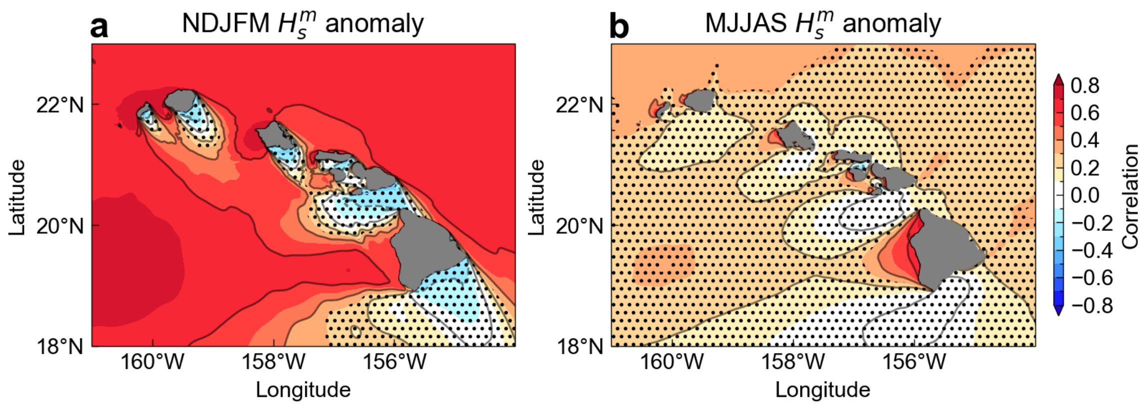

Figure 2. Correlation of mean significant wave height with Niño 3.4 index for November-March and May-September. The contour interval is 0.2. Stippling indicates regions where the correlation is not significant at 95% confidence level (two-tailed Student's t-test).

3 ENSO-based model to reconstruct wave statistics

We develop a semi-empirical model of the climate cycle processes to reconstruct the monthly anomaly of wave statistics W as a function of time t. W can represent H_s^m and are reconstructed as a combination of linear and nonlinear processes based on the ENSO index, accounting for teleconnection of ENSO and its seasonality, as described

$$W(t) = \alpha(t)T_{\mathrm{ENSO}}(t) + \beta(t)T_{\mathrm{ENSO}}^2(t), \tag{1}$$

where $T_{\mathrm{ENSO}}(t)$ is the monthly Niño3.4 index and $\alpha(t)$ and $\beta(t)$ are the seasonally varying linear and nonlinear ENSO forcing coefficients, which can be expressed as $\alpha(t) = \alpha_0\left[1 + A\cos\left(\frac{2\pi}{12}\mathrm{t} + \varphi_{\mathrm{A}}\right)\right]$, and $\beta(t) = \beta_0\left[1 + B\cos\left(\frac{2\pi}{12}\mathrm{t} + \varphi_{\mathrm{B}}\right)\right]$. The parameters A and φ_{A} describe the amplitude and phase of the annual cycle for linear responses; and B and φ_{B} for nonlinear response. The seasonal modulation of the linear forcing coefficient captures the significant difference in the ENSO influence between winter and summer. The nonlinear response in ENSO teleconnections is approximated to second order by a quadratic relation.

Due to the locality-dependent wave conditions around the islands, the parameterization for this ENSO-based wave model is location-specific. As a demonstration, we estimate the linear and nonlinear parameters at buoy #106 off the north shores of Oahu (seen in Figure 1), by multivariate linear regression of the hindcast wave statistics and the observed Niño3.4 from 1980 to 2020. With the optimized parameterization, the H_s^m anomalies can be reconstructed from the ENSO-based model and align well with the wave hindcast to effectively capture inter-annual wave variations (Figure 3). The ENSO-based-wave model provides an effective tool for us to leverage the ENSO long-range predictability to produce the wave forecast on seasonal scales.

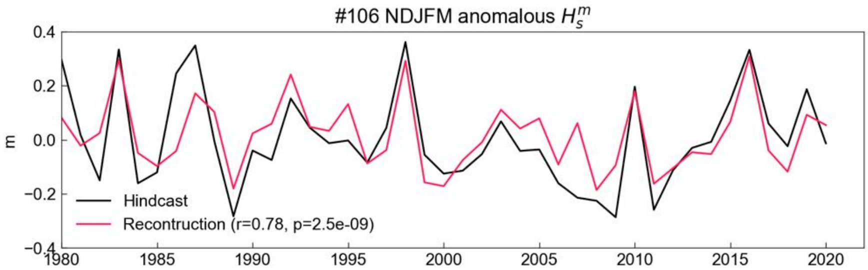

Figure 3. Hs anomalies averaged over November- March at buoy #106 based on wave hindcast (black) and reconstructed using Niño3.4 index (red).

4 Seasonal Wave Forecast

Over the last few decades, great effort has been made to understand ENSO variability and improve ENSO predictability. Recently, the authors developed an extended nonlinear recharge oscillator (XRO) model [11], which integrates core ENSO dynamics with its seasonally modulated interactions with other modes of variability in global oceans. The XRO model demonstrates exceptional performance, with correlations between the observed ENSO3.4 index and its forecasts exceeding 0.7 at a 12-month lead time and remaining above 0.5 at an 18-month lead time. This outperforms global climate models and matches the predictive skill of the most advanced artificial intelligence-based methods.

We applied the XRO ENSO forecasts, instead of the observed Niño3.4 index, to the ENSO-based wave model at buoy #106, which was developed using the high-resolution Hawaii wave hindcast from 1980 to 2009. The forecasted correlation skill is analyzed by comparing the forecasted wave statistics with the wave hindcast from 2010 to 2020. The results in figure 4 shows the forecast correlation, which is averaged over the 10 years by monthly lead time, remains above 0.5 for up to 9 months of lead time. In particular, the target months of December to May have higher forecast skills than other months, due to the strong ENSO influence in winter swells. The promising preliminary results provide a basis to further deploy the ENSO-wave-based model for operational seasonal wave forecasting by leveraging ENSO's robust predictability.

5 Discussion and Conclusions

Hawaii's complex wave climate is shaped by both local and distant weather systems, ranging from mesoscale to synoptic scales. A 42-year high-resolution wave hindcast dataset offers a comprehensive resource for analyzing the spatiotemporal patterns of coastal waves in Hawaii and identifying strong connections between ENSO and wave anomalies. The strong ENSO-wave connections allow us to develop a semi-empirical model to reconstruct seasonal wave statistics for Hawaii. In this pilot study, we implemented the XRO ENSO forecast in the ENSO-based wave model to generate seasonal wave predictions for a selected site on the north shore of Oahu. The wave predictions align well with wave hindcast dataset for lead time up to 9 months. Moving forward, we aim to extend this methodology to the entire coastal waters of the Hawaiian Islands for seasonal-scale wave forecasts. Such forecasts will provide valuable insights for maritime operations, coastal hazard mitigation, and renewable energy harvesting. Furthermore, the framework introduced here can be adapted to other coastal regions in the Pacific Ocean strongly influenced by ENSO.

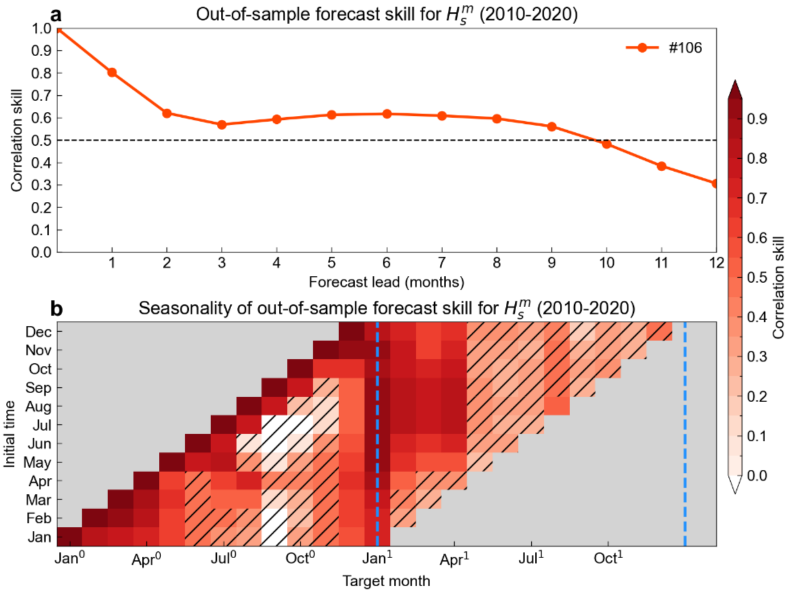

Figure 4. (a) Out-of-sample forecast correlation skill of seasonal mean Hs anomalies over 2010-2020 for buoy #106 using the coupled XRO-wave model, which is trained using the data for 1980-2009. (b) Same as (a) but for the correlation skill as a function of initialization (ordinate) and target months (abscissa; superscripts 0 and 1 denote the current and subsequent years). Hatching highlights forecasts with a correlation skill less than 0.5. The dashed vertical blue lines denote January.

References

[1] Tolman HL. A mosaic approach to wind wave modeling. Ocean Model. 2008;25(1–2):35–47.
[2] Booij N, Ris RC, Holthuijsen LH. A third-generation wave model for coastal regions: 1. Model description and validation. J Geophys Res Oceans. 1999;104(C4):7649–7666.
[3] Saha S, Moorthi S, Wu X, et al. The NCEP Climate Forecast System Version 2. J Clim. 2014;27(6):2185–2208.
[4] Saha S, Moorthi S, Pan H-L, et al. The NCEP Climate Forecast System Reanalysis. Bull Am Meteorol Soc. 2010;91(8):1015–1058.
[5] Skamarock W, Klemp J, Dudhia J, et al. A Description of the Advanced Research WRF Version 3 [Internet]. UCAR/NCAR; 2008 [cited 2024 Dec 30]. p. 1002 KB. Available from: http://opensky.ucar.edu/islandora/object/technotes:500.
[6] Hitzl DE, Chen Y-L, Van Nguyen H. Numerical Simulations and Observations of Airflow through the ‘Alenuihāhā Channel, Hawaii. Mon Weather Rev. 2014;142(12):4696–4718.
[7] Li N, García-Medina G, Cheung KF, et al. Wave energy resources assessment for the multi-modal sea state of Hawaii. Renew Energy. 2021;174:1036–1055.
[8] Boucharel J, Almar R, Kestenare E, et al. On the influence of ENSO complexity on Pan-Pacific coastal wave extremes. Proc Natl Acad Sci. 2021;118(47):e2115599118.
[9] Kumar P, Sardana D, Kaur S, et al. Influence of climate variability on WIND-SEA and swell wave height extreme over the INDO-PACIFIC Ocean. Int J Climatol. 2022;42(12):6183–6203.
[10] Stopa JE, Cheung KF. Periodicity and patterns of ocean wind and wave climate. J Geophys Res Oceans. 2014;119(8):5563–5584.
[11] Zhao S, Jin F-F, Stuecker MF, et al. Explainable El Niño predictability from climate mode interactions. Nature. 2024;630(8018):891–898.